STUDY OF RARE EARTH SUBSTITUTION ON $(K_{0.5}Na_{0.5})NbO_3$ CERAMICS

A PROJECT REPORT

SUBMITTED IN PARTIAL FULFILLMENT OF THE REQUIREMENTS

FOR THE AWARD OF THE DEGREE

OF

MASTER OF SCIENCE

IN

[PHYSICS]

Submitted by

SONAL
2K19/MSCPHY/18

Under the supervision of

DR. RICHA SHARMA

DEPARTMENT OF APPLIED PHYSICS

DELHI TECHNOLOGICAL UNIVERSITY

(FORMERLY Delhi College of Engineering)

Bawana Road, Delhi-110042

MAY, 2021

DELHI TECHNOLOGICAL UNIVERSITY

(FORMERLY Delhi College of Engineering)

Bawana Road, Delhi-110042

CANDIDATE'S DECLARATION

I, **SONAL**, **2K19/MSCPHY/18**, student of M.Sc. (Physics), hereby declare that the project Dissertation titled "**Study of rare earth substitution on $(K_{0.5}Na_{0.5})NbO_3$ ceramics**" which is submitted by me to the Department of Applied Physics, Delhi Technological University, Delhi in partial fulfilment of the requirement for the award of the degree of Master of Science, is original and not copied from any source without proper citation. This work has not previously formed the basis for the award of any Degree, Diploma Associateship, Fellowship or other similar title or recognition.

Place: Delhi   **SONAL (2K19/MSCPHY/18)**

Date: May 31, 2021

CERTIFICATE

I hereby certify that the Project Dissertation titled "**Study of rare earth substitution on** **$(K_{0.5}Na_{0.5})NbO_3$**" which is submitted by **SONAL, (2K19/MSCPHY/18)** [Department of Applied Physics]. Delhi Technological University, Delhi in partial fulfilment of the requirement for the award of the degree of the Master of Science, is a record of the project work carried out by the student under my supervision. To the best of my knowledge this work has not been submitted in part or full for any Degree or Diploma to this University or elsewhere.

Place: Delhi   **Dr. Richa Sharma**

                                                                 (Assistant Professor)

Date: May 31, 2021   **SUPERVISOR**

PLAGIARISM REPORT

turnitin

Sonal

project_report 222.pdf

Sources Overview

6%
OVERALL SIMILARITY

1	A. Mayeen, N. Kalarikkal. "Development of ceramic-controlled piezoelectric devices for biomedical applications", Elsevier BV, 2018 CROSSREF	**1%**
2	coek.info INTERNET	**<1%**
3	pubs.rsc.org INTERNET	**<1%**
4	Savitribai Phule Pune University on 2019-05-02 SUBMITTED WORKS	**<1%**
5	Jie Xing, Shaoxiong Xie, Bo Wu, Zhi Tan, Laiming Jiang, Lixu Xie, Yuan Cheng, Jiagang Wu, Dingquan Xiao, Jianguo Zhu. "Influence of different lan... CROSSREF	**<1%**
6	Jigong Hao, Wei Li, Jiwei Zhai, Haydn Chen. "Progress in high-strain perovskite piezoelectric ceramics", Materials Science and Engineering: R: Rep... CROSSREF	**<1%**
7	scholarbank.nus.edu.sg INTERNET	**<1%**
8	Li, Jing-Feng, Ke Wang, Fang-Yuan Zhu, Li-Qian Cheng, and Fang-Zhou Yao. "(K,Na)NbO3 -Based Lead-Free Piezoceramics: Fundamental Aspects, ... CROSSREF	**<1%**
9	Haibibu Aziguli, Tao Zhang, Ping Yu. "Effect of Additive Glycerol on Piezoelectric Properties of Modified Sol-Gel (Ba$_{0.85}$Ca$_{0.15}$... CROSSREF	**<1%**
10	Cheol-Woo Ahn. "Low Temperature Sintering and Piezoelectric Properties of CuO-Doped (K0.5Na0.5)NbO3 Ceramics", Ferroelectrics Letters Secti... CROSSREF	**<1%**
11	University of New South Wales on 2018-07-26 SUBMITTED WORKS	**<1%**
12	"Piezoelectric Motor Technology: A Review", Nanopositioning Technologies, 2016. CROSSREF	**<1%**
13	Higher Education Commission Pakistan on 2016-09-29 SUBMITTED WORKS	**<1%**
14	Jing-Feng Li. "Lead-Free Piezoelectric Materials", Wiley, 2021 CROSSREF	**<1%**
15	Sheffield Hallam University on 2019-09-16 SUBMITTED WORKS	**<1%**
16	The University of Manchester on 2008-12-12 SUBMITTED WORKS	**<1%**

Excluded search repositories:
- None

Excluded from Similarity Report:
- Bibliography
- Quotes
- Small Matches (less than 10 words).

Excluded sources:
- None

DEPARTMENT OF APPLIED PHYSICS

DELHI TECHNOLOGICAL UNIVERSITY

(FORMERLY Delhi College of Engineering)

Bawana Road, Delhi-110042

<u>ABSTRACT</u>

One of the greatest issues that the world has faced in recent decades is the energy crisis. Overpopulation, unsustainable use of non-renewable sources of energy, old and inadequate technology of power generating equipment, and misuse of available energy sources such as fuel, electricity, and so on have all contributed to an alarming increase in global energy consumption. Energy harvesting from other sources of energy is becoming increasingly important in order to meet demand, and substantial research is ongoing to find a sustainable solution to the problem of energy crisis. Piezoelectric Energy harvesters have the potential to be integrated into a wide range of human-powered applications, making it a feasible answer to our growing energy demands. The development of new sensors, actuators, and transducers requires the use of functional piezoelectric materials. PZT based piezoelectric materials outperform other multifunctional ceramics in terms of piezoelectric and ferroelectric features. However, due to the toxicity of lead, the usage of PZT ceramics has been strictly restricted. As a result of which new lead-free piezoelectric materials with excellent piezoelectric and ferroelectric characteristic are required. Recent research on Pb-free piezoelectric materials such as $BaTiO_3$ (BT), $(Bi,Na)TiO_3$ (BNT), and $(K,Na)NbO_3$ (KNN) has discovered that Pb-free systems can attain good piezoelectric and ferroelectric characteristics. Out of which KNN ceramics showed great promising

properties but due to the low evaporation temperature of Na and K, KNN-based ceramics are difficult to sinter. Special additives must be introduced in KNN-based ceramics to inhibit these volatiles from evaporating and to lower the sintering temperature. Enhanced functionality of KNN-based ceramics can be achieved by adding different dopants such as $(K,Na)NbO_3$–$BaTiO_3$, $(K,Na)NbO_3$–$LiSbO_3$, $(K,Na)NbO_3$–$LiNbO_3$, $(K,Na)NbO_3$–$SrTiO_3$, $(K,Na)NbO_3$–$LiNbO_3$–$AgTaO_3$, and $(K,Na)NbO_3$–$LiTaO_3$, which results in KNN-based ceramics with better densification properties. Modification of KNN-based piezoceramics via doping rare-earth ions is a very effective way to enhance properties among other doping ions.

So in this study, we chose rare earth metal Ho as dopant and fabricated Ho^{3+} doped $(K_{0.5}Na_{0.5})NbO_3$ ceramic via solid-state reaction method to examine the effect of rare-earth on phase structure of $(K_{0.5}Na_{0.5})NbO_3$ piezoceramics.

DEPARTMENT OF APPLIED PHYSICS

DELHI TECHNOLOGICAL UNIVERSITY

(FORMERLY Delhi College of Engineering)

Bawana Road, Delhi-110042
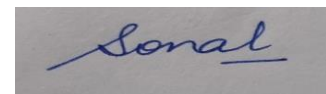
ACKNOWLEDGEMENT

I have taken efforts in this project. However, it would not have been possible without the kind support and help of many individuals. I would like to extend my sincere thanks to all of them.

I would like to express my sincere gratitude and deep appreciation to my esteemed guide **Dr. Richa Sharma,** Assistant Professor, DTU, for her guidance and constant supervision as well as for providing necessary information regarding the project and also for their support in completing the project.

I would like to extend my deepest gratitude to **Ms. Komal Verma,** Research Scholar, DTU, for helping me while performing the experiments and also her invaluable discussions on several topics that provided me a good understanding of the topics.

I would like to express my gratitude towards my parents and my friends for their kind cooperation and encouragement which helped me a lot in completion of this project.

In addition, I would like to thank Department of Applied Physics, Delhi Technological University for giving me the opportunity to work on this topic.

SONAL

CONTENTS

LIST OF TABLES AND FIGURES

LIST OF SYMBOLS

Letter name	Uppercase	Lowercase	Letter name	Uppercase	Lowercase
Alpha	A	α	Nu	N	ν
Beta	B	β	Xi	Ξ	ξ
Gamma	Γ	γ	Omicron	O	o
Delta	Δ	δ	Pi	Π	π
Epsilon	E	ε	Rho	P	ρ
Zeta	Z	ζ	Sigma	Σ	σ
Eta	H	η	Tau	T	τ
Theta	Θ	θ	Upsilon	Υ	υ
Iota	I	ι	Phi	Φ	φ
Kappa	K	κ	Chi	X	χ
Lambda	Λ	λ	Psi	Ψ	ψ
Mu	M	μ	Omega	Ω	ω

LIST OF ABBREVIATIONS

BT- Barium Titanate

PZT- Lead Zirconium Titanate

KNN- Potassium Sodium niobate

GPS- Global Positioning System

PEGs- Piezoelectric Generators

MPB- Morphic Phase Boundary

PPT- Polymorphic Phase Boundary

XRD- X-Ray Diffraction

PDE- Powder Diffraction File

ICPD- International Centre for Diffraction Data

JCPDS- Joint Committee on Powder Diffraction Standards

CHAPTER 1

INTRODUCTION

1.1 Ferroelectricity

Ferroelectricity is discovered by J. Valasek in 1921 while researching the dielectric characteristics of Rochelle salt ($NaKC_4H_4O_6.4H_2O$) [1]. Ferroelectricity is a subtype of pyroelectricity that shows spontaneous polarisation below the Curie temperature. By introducing an electric field to ferroelectric materials, this spontaneous polarisation can be reoriented; total polarisation reversal is referred to as "switching" (shown in fig. 1.1). The crystal symmetry of the materials determines the direction of spontaneous polarisation, which is most important below the Curie temperature [2]. A ferroelectric material is typically single crystalline or polycrystalline, with spontaneous reversible polarisation over a range of temperature. The Curie temperature, at which the ordered to disordered phase transition occurs, is a critical temperature. At this temperature, the dielectric constant may be higher than in the disordered phase. Ferroelectric crystals or crystallites must be non-centrosymmetric because the order to disorder phase transition necessitates atom displacement. This indicates that a transition of phase will result in mechanical strain, altering the shape and volume of the material body, as well as its optical refractive index. As a result, ferroelectric systems possess not just the ferroelectric but can also piezoelectric, electro-optic, and pyroelectric phenomena, making them useful in a wide variety of technical applications [3]. In the 1950s, more study into ferroelectric materials resulted in the discovery of barium titanate ($BaTiO_3$), which is possibly the most well-known ferroelectric substance. It's a ceramic that's often utilised in capacitors and piezoelectric transducer devices. Since then, several more ferroelectric oxides with high electromechanical coupling coefficients and dielectric constants have been discovered, including tungsten bronze, pyrochlore, perovskite, and bismuth titanate layer structures [1].
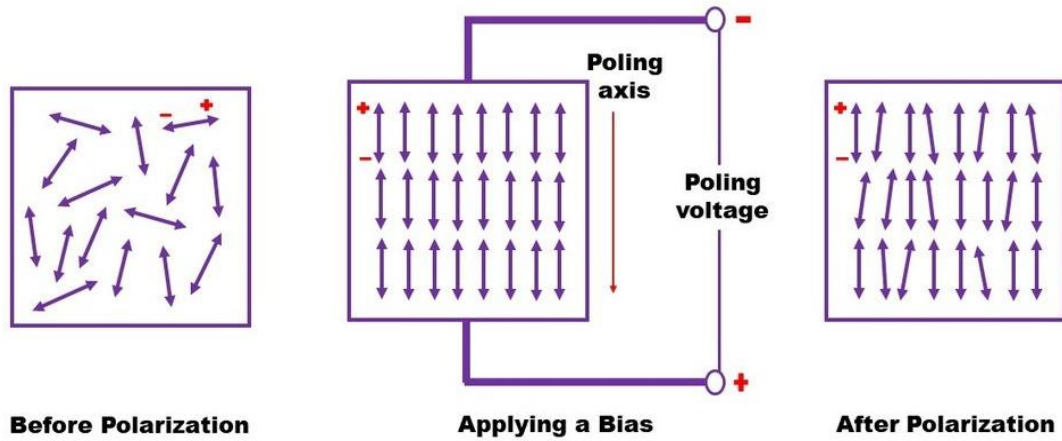
Fig. 1.1 Behaviour of ferroelectric materials under application of electric field.

1.2 Piezoelectricity

The Curie brothers discovered the piezoelectric phenomenon in 1880 and named it piezoelectric effect. In this phenomenon, when a mechanical stress or force is applied on piezoelectric materials there will be the generation of electrical signals. Some crystalline materials with non-centre-symmetries have a unique feature called piezoelectricity. Piezoelectric effects, such as the direct piezoelectric effect in which there is the generation of electric polarisation through the application of mechanical stress and the converse piezoelectric effect in which there is the generation of mechanical strain through the application of an electric field (illustrated in fig. 1.2), are important in a variety of electronic devices, including actuators, sensors, and transducers [4][5].
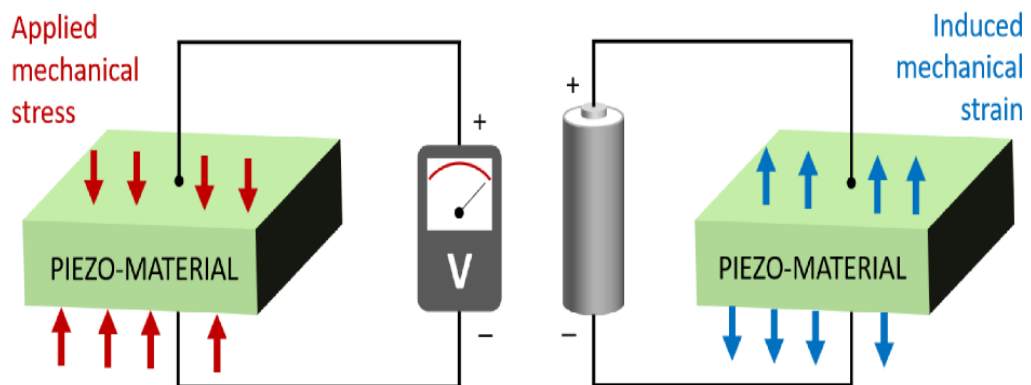

Fig. 1.2 Direct and Converse piezoelectric effect.

When a piezoelectric is connected in a circuit, electrical dipoles within the material create the electric output or potential difference across the material. Whenever the material is not stressed, it is neutrally charged, which means the opposite charges within it balance one other, the electric dipoles cancel out each other, and no electrical output is produced. It is subjected to stress when an external force is applied on them. The equation for stress is given below,

Stress = Force/ Cross-section area   (1.1)

As a result of the stress, the relative positions of the charges with respects to each other change, resulting in a change in the moment of dipole. There is a potential difference within the material since the charges do not cancel each other. As a result of the stress, the material will deform. When a material deforms, it tends to build positive charge on one end and negative charge on the other; the potential difference created permits the charges to travel across the circuit, resulting in the generation of electricity.

When a potential difference is supplied across a material, electrostatic attraction or repulsion is produced by either like or opposite charges, resulting in a change in charge position, which is known as the converse piezoelectric effect or the inverse piezoelectric effect. This is due to variations in the electric dipole moment. [6]. These effects are illustrated in fig. 1.3.

(a)   *(b)*
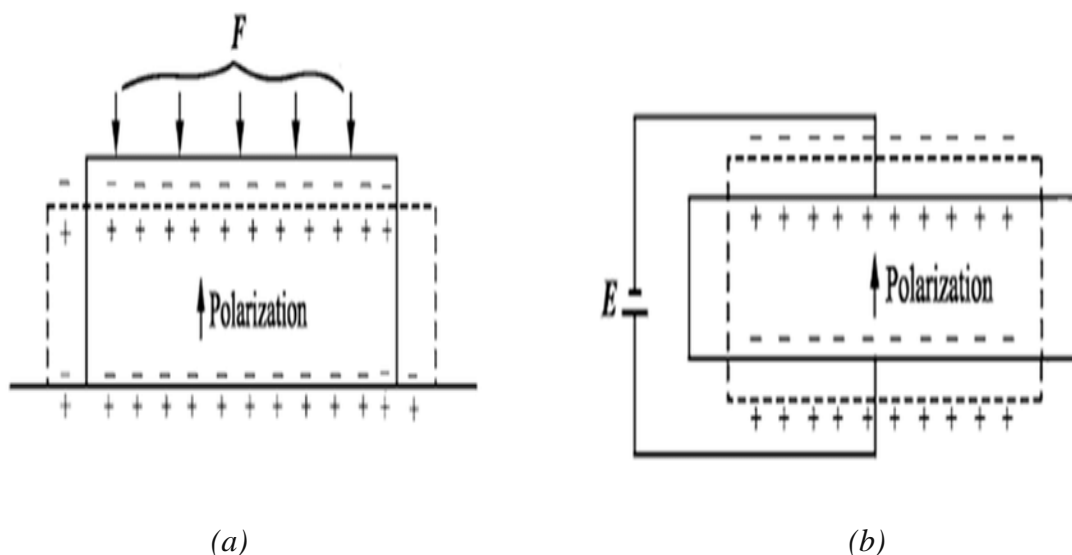
Fig. 1.3 (a) Stress causes the crystal lattice to distort, resulting in an electric dipole. (b) An applied electric field, on the other hand, causes the lattice to distort as a result.

The piezoelectric effect is seen in 20 of the 32 crystal classes and is always found in the crystals those do not have a centre of symmetry. Because of their crystalline form, naturally occurring minerals like quartz and berlinite display this effect. The piezoelectric activity of man-made synthetic materials like PZT and BT is imparted by a process known as poling. The most commonly studied ferroelectric systems include perovskite, ilmenite, bismuth-layer, and tungsten bronze structure ferroelectrics [5]. All ferroelectrics are piezoelectric but all piezoelectric are not ferroelectrics. And all ferroelectric materials are pyroelectrics but all pyroelectric materials are not ferroelectrics [1]. The relationship is illustrated in fig. 1.4.
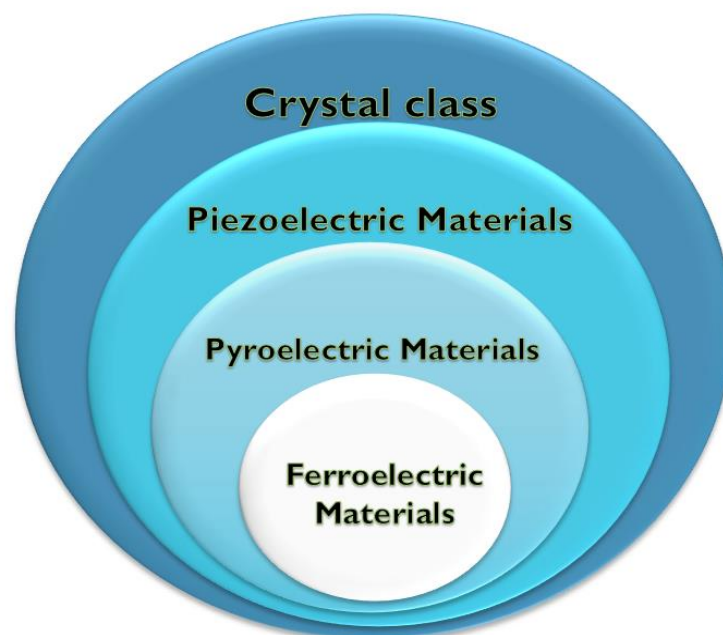
Fig. 1.4 Relationship between Piezoelectric, Pyroelectric, and Ferroelectric materials.

1.3 Piezoelectric Energy Harvesting

With fast urbanisation and industrial growth, need for fossil fuels such as coal, natural gas and petroleum is rising. However, fossil fuels are non-renewable resources that produce a significant quantity of pollution and waste. As a result, developing renewable sources of energy as alternative to the conventional fossil fuels is very important [7]. Even if many natural energy sources, such as solar, wind power, and hydro can reduce energy consumption, they are heavily influenced by environmental conditions and are therefore unsuitable for indoor operations. As a result, energy harvesting from waste

mechanical energy such as vibrations, human motion, biomechanics, walking, running, wind, flow of water, and so on, is a potential strategy that might be used to generate renewable, sustainable and portable energy [8]. With the expansion of human civilization and the rapid growth of science and technology, portable microelectronic gadgets have become increasingly popular. The sources of energy for these gadgets have been a significant topic of study [7]. Various techniques, like piezoelectric effect, electrostatic production, and electromagnetic induction have been developed to convert enormous mechanical energy into useful electricity. Piezoelectric generators (PEGs) recently gotten a lot of attention because of their direct power conversion abilities and very simple fabrication [8]. Mechanical strain is converted to electrical voltage by the piezoelectric effect. This strain might come from a variety of sources. A few examples include human motion, acoustic noise, and low-frequency earthquake tremors. Walking can be used to harvest mechanical energy using the piezoelectric effect. This energy can be transformed into usable electrical energy, which can be utilised to power wearable electronic equipment such as sensors and GPS receivers [9]. Energy harvesting using piezoelectric materials is called piezoelectric Energy harvesting. Steps include in piezoelectric energy harvesting are illustrated in fig. 1.5.
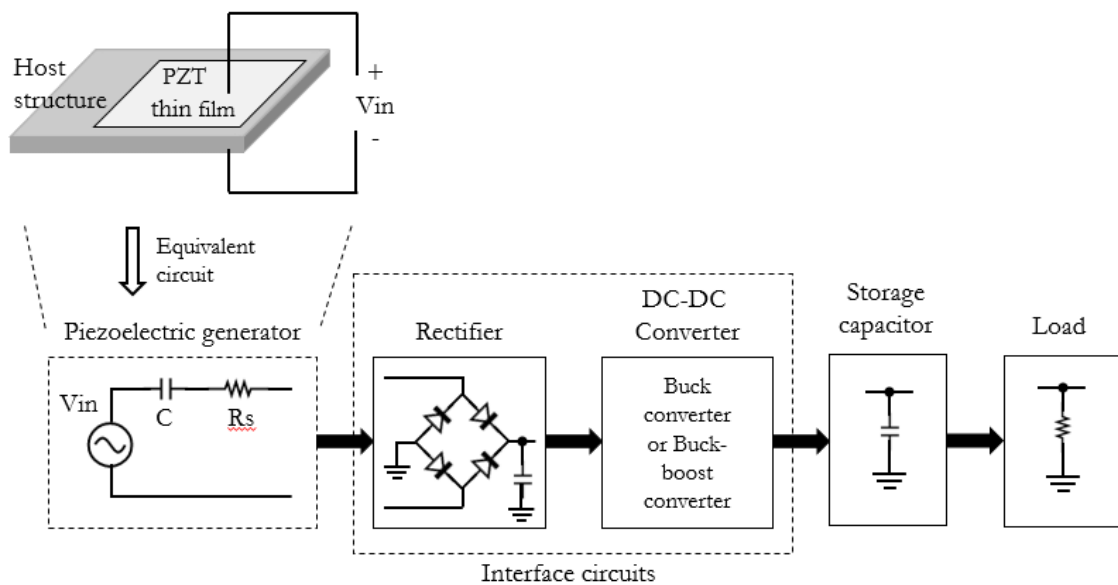

Fig. 1.5 Block diagram of energy harvesting using piezoelectric.

Piezoelectric energy harvesters are commonly used in shoes, anti-lock brake systems, synthetic pacemakers, and bridge and buildings monitoring equipment (as shown in fig. 1.6) [10].
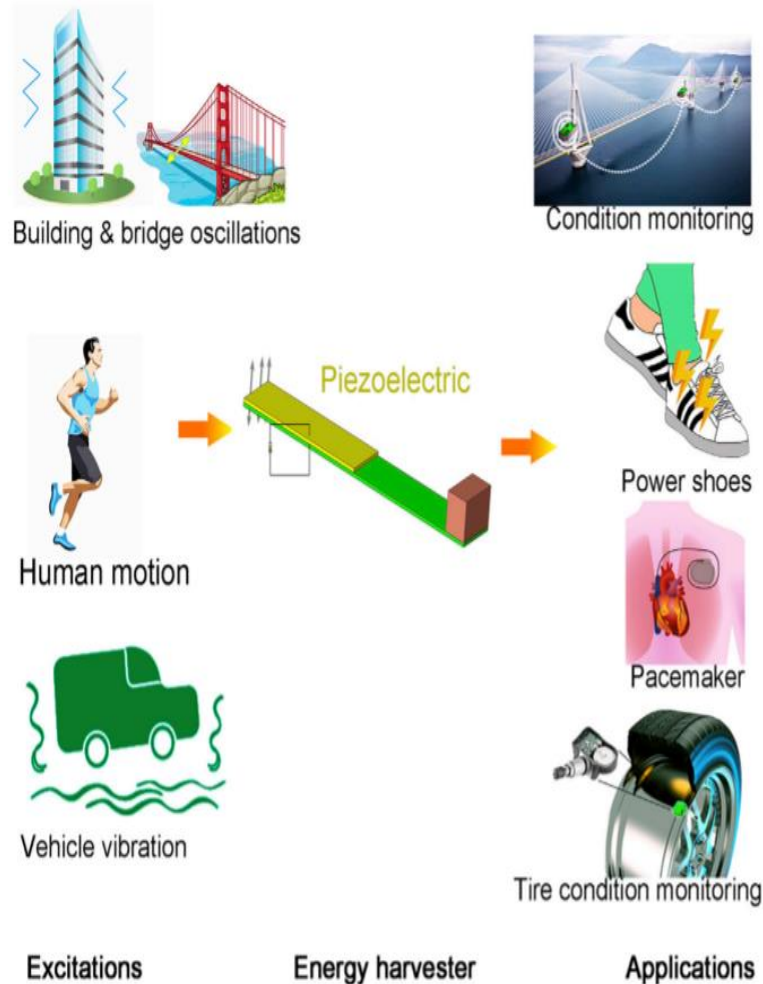
Fig. 1.6 Some basic applications of Piezoelectric Energy Harvesters.

For efficient power generation based on multiple categories of piezoelectric energy harvesters, such as ceramic materials, and poly vinylidene fluoride (PVDF) and its copolymers, a variety of PEGs with varied function and structure have been produced [8]. Barium titanate (BaTiO$_3$) is first ever piezoelectric material in piezoelectricity which was discovered in 1946, resulting in a rapid advancement in piezoelectric materials. PZT (Lead zirconium titanate) ceramics, which exhibit greater piezoelectricity than BaTiO$_3$, were found by Jaffe B et al. in 1954 [11]. Lead zirconium titanate abbreviated as PZT has the formula (1-x)PbTiO3-xPbZrO3 or Pb(Zr$_{1-x}$Ti$_x$)O3, was regarded as a major milestone in piezoelectric science in the 1950s. Earlier lead-based ceramics such as lead zirconium

titanate (PZT) with high piezoelectric properties considered as the most promising piezoelectric materials. As is generally known, Pb is a highly hazardous substance that can harm the humans as well as other living organisms. The most harmful Pb has been released into the environment as a result of increased utilisation of PZT. As a result, foreign authorities have enacted legislation limiting the use of Pb-based materials in the manufacture of a wide range of products [12]. Due to which the researchers started focusing on finding lead-free piezoceramics, new materials such as $(K_{0.5}Na_{0.5})NbO_3$ (KNN) and $(Bi_{0.5}Na_{0.5})TiO_3$ (BNT) have resulted [13][14]. The strong ferroelectricity of Pb-free $(Bi_{0.5}Na_{0.5})TiO_3$ (BNT) ceramics was discovered in 1960 [4]. Before the twenty-first century, lead-free piezoelectric materials had little advancements in electrical properties. However, since the beginning of the twenty-first century, the Pb-free perovskite ceramics such as KNN, BT, and BNT have gotten a lot of attention because of considerable improvements in their physical properties [15]. The most commonly explored lead-free systems among the numerous options are KNN, BNT, and BT based perovskite materials.

Perovskites have been created as the most successful and sustainable energy resources for a variety of optoelectronic and photonic device applications. Every material which has the crystal structure identical to the material perovskite, which is composed by calcium titanium oxide ($CaTiO_3$), is referred to as a perovskite which was discovered by Perovski [16]. Perovskite mineral ($CaTiO_3$) has an orthorhombic structure with space group *Pbnm*. Many compounds with the formula ABX_3 show the cubic perovskite structure, where A and B are cations with distinct oxidation values and X is an anion. The A-cation is located in the unit cell's centre, whereas the B cation and X anions are located in the unit cell's corners and edges, respectively (shown in fig. 1.7) [12]. Perovskite materials' unusual physical features, such as high absorption coefficient, ferroelectric characteristics, low exciton-binding energy, long-range ambipolar charge transfer, high dielectric constant, and so on, have sparked a lot of interest in optoelectronic and photovoltaic applications [16].
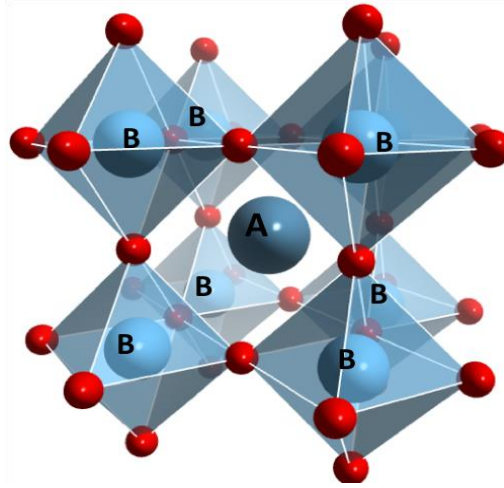
Fig. 1.7 The perovskite structure, with A & B as positively charged ions, and the red spheres representing oxygen atoms.

A number of studies have recently been published that summarise the present state of research on these lead-free piezoelectric compositions. KNN perovskite is a dominant lead-free alternative with a high Curie temperature and good piezoelectric and ferroelectric characteristics among these materials [17]. High piezoelectric coefficient ($d_{33} \approx 416$ pC/N) was attained in KNN-based ceramics with phase boundary of orthorhombic-tetragonal (O-T) manufactured using the reactive template grain growth (RTGG) process in 2004. By creating new phase boundaries of rhombohedral (R) and tetragonal (T) phases, a variety of KNN-based ceramics of high piezoelectric constants ($d_{33} = 490$–570 pC/N) were achieved 10 years later (2014). Following that, by producing textured KNN-based ceramics, ultrahigh piezoelectric coefficient d_{33} of 700 pC/N and huge k_p of 0.76 were reported [4].

KNN is a perovskite material with ABO_3 structure in which A-site is take up by K and Na cations and B-site is take up by Nb anion. At ambient temperature, KNN is a solid mix of ferroelectric $KNbO_3$ with space group Cm2m and antiferroelectric $NaNbO_3$ with space group Pbma with an orthorhombic perovskite structure [18]. KNN is believed to have an orthorhombic structure with the space group Amm2 at room temperature (as shown in fig. 1.8).
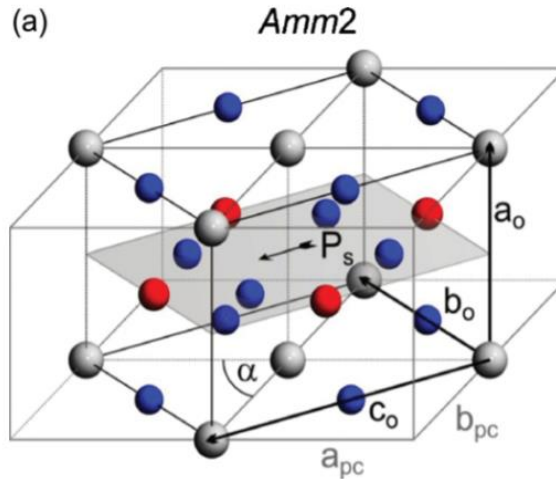
Fig. 1.8 The Orthorhombic structure with space group Amm2 of KNN [19].

KNN experiences many phase transitions similar to KN at higher temperatures, with two phase changes found above room temperature: an orthorhombic to tetragonal phase change at low temperature and a tetragonal to cubic phase change at high temperature. [20]. In the low temperature region of KNN ceramics, three types of phase transition such as rhombohedral to orthorhombic ($T_{R–O}$), orthorhombic to tetragonal ($T_{O–T}$), and rhombohedral to tetragonal ($T_{R–T}$) phase transition temperature occur, which are commonly referred to as polymorphic phase transitions (PPT) [21]. Because of its superior ferroelectric and piezoelectric capabilities, the composition at x = 0.5 is of particular interest.   Rhombohedral-orthorhombic ($T_{R–O}$) at 110 °C, orthorhombic-tetragonal ($T_{O–T}$) at 180 °C, and tetragonal-cubic ($T_{T–C}$) at 400 °C are the three phase transitions in $K_{0.5}Na_{0.5}NbO_3$ [22] [23].

 As the preparation of KNN-based ceramics is simple, so the study of these ceramics is easy and predominant. However, it has been observed that at high temperature, K and Na volatilize from the A-site, causing a shift in the K, Na, and Nb stoichiometry ratio in these ceramics. Intrinsic defects and oxygen vacancies occur as a result of volatilization, resulting in a decrease in the electrical properties of pure KNN ceramics. Divergence of KNN from stoichiometry also facilitates the development of secondary phases and makes difficult to obtain dense KNN ceramics [18]. As a result, many approaches to achieving temperature stability have been considered. We can achieve temperature stability by improving the structure of KNN or adding different cations (dopants) to the A and B-site of the KNN compound. Furthermore, existence of MPB (morphotropic phase boundary)

results in enhanced piezoelectric ceramic properties [24]. In KNN-based ceramics, it is observed that by getting PPT (i.e., polymorphic phase transition) temperature close to room temperature enhanced properties could be achieved. Therefore, many high performance KNN-based ceramics were synthesised by constructing phase boundary close to room temperature [25].

From various dopants the rare earth ion doping in KNN-based ceramics is a very efficient way to enhance the properties of piezoceramics. Just a few studies have been reported to examine the effect of rare-earth substitution on the KNN-based piezoceramics. Rare earth metal ions doped in KNN inhibit K and Na (alkali metal) ions from volatilizing, improving piezoelectric properties and temperature stability. Furthermore, doping rare earth metal ions in KNN reveals the concurrence of orthorhombic and tetragonal phases near ambient temperature, resulting in improved properties of piezoelectric materials due to the polymorphic phase transition (PPT) [25]. Doped rare earth metals have a radius similar to that of the host Na^+ and K^+, and will take up the A-site of the ABO_3 perovskites, which will decrease as the number of atomic of rare earth metals increases. This lowers the concentration of oxygen vacancies and decreases intrinsic defects and hence the temperature stability of KNN piezoceramics can be achieved [26]. Moreover, as the ionic radius is decreased, the grain size increases at first, then decreases after reaching a limit in Nd-doped ceramics. The microstructure of ceramics has a major effect on their properties. Increased grain growth can improve properties by making domain switching easier, while smaller grains can intensify the coupling effect between grains and grain boundaries, making domain switching more difficult [24]. Doping Pr^{3+} ions into $(K_{0.5} Na_{0.5})NbO_3$ ceramics increases the piezoelectric constant d_{33} to 108.4 pC/N, which is 1.25 times more than that of pure KNN ceramics. In addition, Er^{3+}, Nd^{3+}, Dy^{3+} and Ho^{3+} are doped in KNN-based ceramics to achieve enhanced properties. The Nd^{3+} doped KNN ceramics shows good properties such as $T_c = 223$ $^\circ$C, $d_{33} = 400$ pC/N, and $k_p = 0.46$ [27].

In this work, intermediate rare earth metal Ho is doped in KNN-based ceramics to study the enhanced piezoelectric properties, as the piezoelectric properties of these ceramics have not been studied yet.

CHAPTER 2

SYNTHESIS PROCESS AND CHARACTERIZATION TECHNIQUES

2.1 Steps of Solid-State Reaction Route

```
Raw Materials → Mixing → Ball Milling → Grinding
                                              ↓
Characterization ← Electroding ← Sintering ← Pellet Formation ← Calcination
```
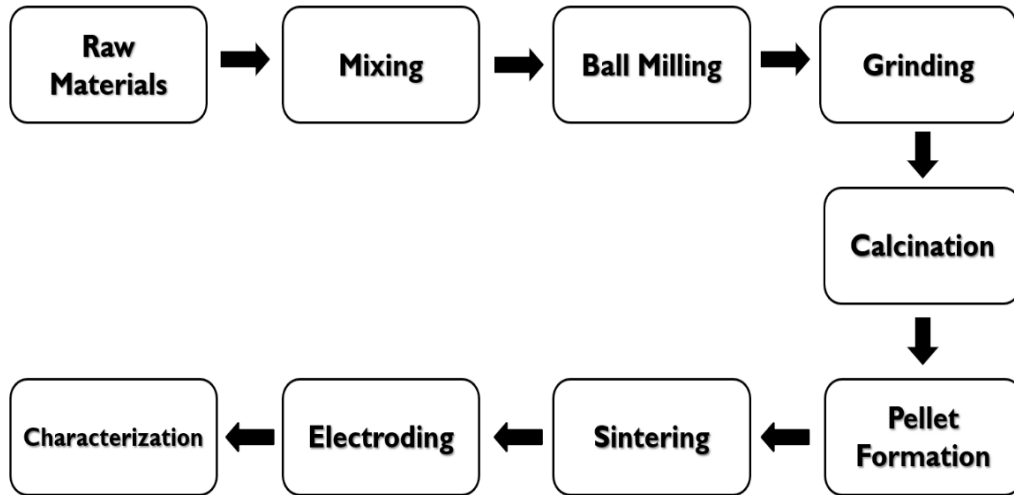
Fig. 2.1 Flowchart of the solid-state fabrication process of ceramics.

Solid State Reaction Method

A typical synthesis method for obtaining polycrystalline material from solid chemicals is solid-state reaction. A very high temperature is frequently used to initiate the reaction. At room temperature, the solids do not naturally react with each other and must be heated to a considerably higher temperature. Chemical and morphological features of the reagents, such as surface area, reactivity, and free energy change with the solid-state reaction, as well as other reaction parameters, such as pressure, temperature, and the reaction environment, are all factors that influence the solid-state reaction [28]. The initial components in a typical synthesis technique are oxide precursors. The needed amount of raw chemicals is weighed and grinded to a fine powder using Ball Milling. During the mixing process, the reaction begins spontaneously, accompanied by the production of heat and water vapour. Acetone and alcohol are sometimes used as mixing medium in order to achieve a uniform mixture [29]. The steps are as follows (as shown in fig. 2.1);

Raw materials

Raw material such as metal oxides and carbonates are first weighed according to the stoichiometric formula. The purity of the raw materials should be good. The particle size of the powder should be in the range of submicron.

Mixing

Reactants are mixed after they have been weighed according to their stoichiometric ratios in the chemical equation. Mechanical mixing is done by Ball Milling.

Ball Milling

Ball milling is a powder-processing technique that is primarily used for particle size reduction and the mixing of different raw material [30].

Calcination

Calcination is the heating of a substance at a specific temperature and in a specific atmosphere. Heating a substance to a high temperature below its melting or fusing point, resulting in reduction or oxidation, moisture loss, and dissociation into simpler compounds. The higher the calcination temperature, the better the final ceramic product's uniformity and density. To obtain the finest electrical and mechanical qualities, a proper calcination temperature is required. Our goal in the calcination process is to remove water and CO_2 in order to generate the necessary solid solution and, as a result of the reaction, to have less volume shrinkage in the final firing. Calcination process is done in furnace.

Grinding

An agate mortar pestle is used to grind lumps created by calcination.

Binder Addition

To make dense ceramic pellets, PVA (Polyvinyl alcohol) binder is added to the calcined powder. Also, it provides strength to the green body.

Shaping

Pellets of the ceramic powder are made using die set by Hydraulic press machine (as shown in fig. 2.2).

Fig. 2.2 Pellet formation by Hydraulic Press Machine using die set.

Binder Burn Out

Formed pellets then heated at 600 °C for 2 hours to volatize PVA binder from them in hot air oven (shown in fig. 2.3).

Fig. 2.3 Hot air oven.

Sintering

Sintering is a thermal technique that uses heat and/or pressure to turn loose tiny particles into a solid coherent mass without melting them completely. Sintering duration, pressure, atmosphere, temperature, and heating/cooling rates are all critical elements that must be tuned in order to achieve the appropriate degree of bonding between the particles, resulting in maximum densification as well as better physical and mechanical qualities [31].

2.2 Advantages of solid-state reaction route

The ease and large-scale production are two advantages of the solid-state reaction approach [28]. The solid-state route is less expensive and requires less complicated equipment. Furthermore, large quantities of powder can be made in a relatively straightforward method [32]. This method is also safe for the environment.

2.3 Experimental Procedure

Sample preparation (host-KNN)

The following approach was used to make 20 g of $(K_{0.5}Na_{0.5})NbO_3$ according to the chemical reaction below. The masses of the reactants were determined using 20 g of the target product. The chemical reaction is as follows:
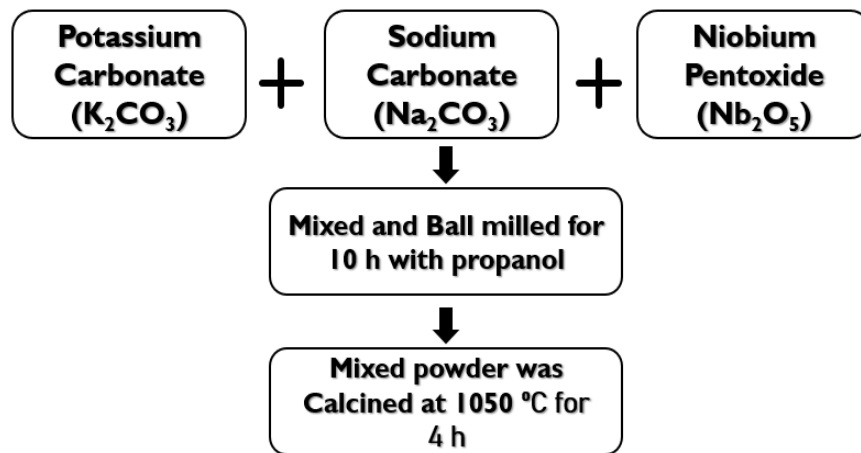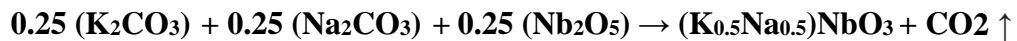
$$0.25 \ (K_2CO_3) + 0.25 \ (Na_2CO_3) + 0.25 \ (Nb_2O_5) \rightarrow (K_{0.5}Na_{0.5})NbO_3 + CO2 \uparrow$$

Fig. 2.4 Synthesis route of $K_{0.5}N_{0.5}NO_3$ by solid-state reaction.

Procedure

Stoichiometric ratios are computed using chemical reactions as a basis. The masses of the reactants K_2CO_3, Na_2CO_3, and Nb_2O_5 are estimated using the theory that the reactant and product sides should be equal. Here we need 20 g of $(K_{0.5}Na_{0.5})NbO_3$. The raw chemicals K_2CO_3 (99% purity), Na_2CO_3 (99% purity), and Nb_2O_5 (99% purity) were weighed in stoichiometric ratio, mixed and Ball milled with propanol for 8 hours, zirconia balls used as grinding media. After mixing the powder was dried at 65 ºC for 10 hours, then calcined at 1050 ºC in alumina crucible for 4 hours in air (as shown in fig. 2.5). Calcined powder then mixed with binder solution of 2wt% polyvinyl alcohol

(PVA) and pressed into pallets by hydraulic press machine. The X-ray diffraction (XRD) data of calcined powder of KNN was collected using an automated diffractometer.

Fig. 2.5 Calcined white powder of $K_{0.5}Na_{0.5}NbO_3$.

Sample preparation (KNN-Ho)

We choose to synthesize the host with Ho^{3+} doping after determining the calcination using XRD of the undoped host. The $K_{0.5}Na_{0.5}NbO_3$ (KNN) ceramics doped with x wt% Ho (abbreviated as KNN: Ho-x, x=0, 0.1, 0.5, 1, 2, 4) were synthesised via solid state reaction. Here we want 5g of each sample. The raw chemicals K_2CO_3, Na_2CO_3, Nb_2O_5, and Ho_2O_3 were weighed in stoichiometric ratio, mixed and ball milled with propanol for 10 hours, zirconia balls used as grinding media. After mixing the mixed powders were dried at 65 ºC for 10 hours, then calcined at 1050 ºC in alumina crucible for 4 hours in air. Each calcined mixture then mixed with a binder solution which is 2wt% of polyvinyl alcohol (PVA) and then compressed into pallets by hydraulic press machine. The X-ray diffraction (XRD) data of calcined powder of Ho doped KNN were collected using an automated diffractometer.

Table 1. Concentration of raw materials used in the synthesis of KNN-Ho.

x wt% Ho	Ho$_2$O$_3$ (g)	K$_2$CO$_3$ (g)	Na$_2$CO$_3$ (g)	Nb$_2$O$_5$ (g)
0	0	1.0046	0.7704	3.8646
0.1	0.005	1.0036	0.7697	3.8608
0.5	0.025	0.9996	0.7666	3.8453
1	0.05	0.9946	0.7627	3.826
2	0.1	0.9846	0.755	3.7873
4	0.2	0.9645	0.7396	3.71

Potassium Carbonate (K$_2$CO$_3$) + Sodium Carbonate (Na$_2$CO$_3$) + Niobium Pentoxide (Nb$_2$O$_5$) + Holmium Oxide (Ho$_2$O$_3$)

Mixed and Ball milled for 10 h with propanol

Various mixed powders with different concentration of Ho in KNN were Calcined at 1050 ℃ for 4 h
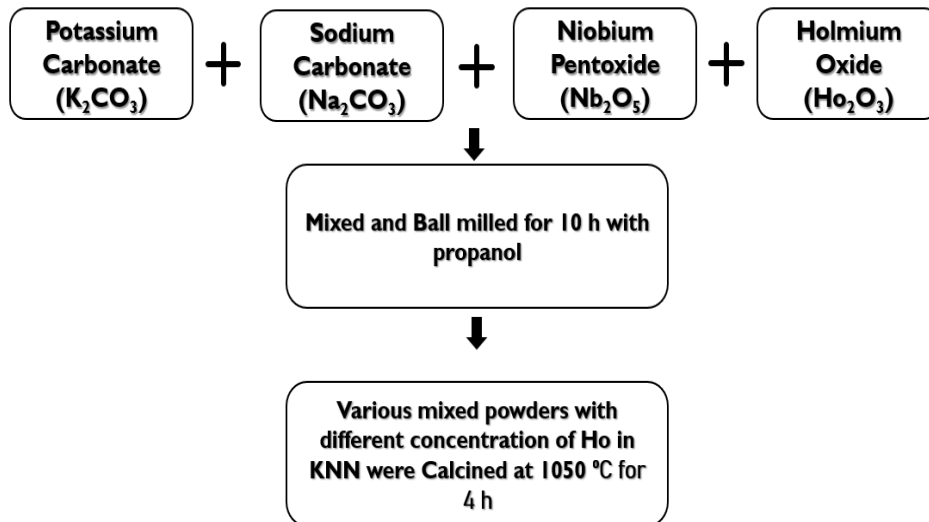
Fig. 2.6 Synthesis route of Ho doped K$_{0.5}$N$_{0.5}$NO$_3$ by solid-state reaction.

2.4 Characterization Techniques

2.4.1   X-Ray Diffraction

One of the most essential materials characterisation technologies is X-ray diffraction (XRD). Characterization of crystalline materials using X-ray diffraction (XRD) is a strong non - destructive method. Crystal structure, crystal orientation, phase, and many other structural characteristics such as particle size, stress, and crystal imperfections are

all provided by XRD. When the beam of monochromatic source of X-rays are diffracted by the planes of lattice at certain angles, then the XRD peaks are formed by constructive interference. The intensity of peaks is determined by the atomic arrangement within the crystal lattice [33].

Fig. 2.7 X-Ray Diffractometer.

XRD is the flexible scattering of photons of x-ray by the atoms present in the lattice. Based on Bragg's law, single-color x-rays that are in phase and distributed cause constructive interference. Bragg's law is given as (shown in fig. 2.8),

$$2d\sin\theta = n\lambda \tag{2.1}$$

Here λ is the wavelength, θ is the angle between the beam which is incident and the normal to the lattice where reflection has taken place, *n* is the order of reflection (an integer) and *d* is the spacing in the crystal planes. Every angle of each crystallographic phase is measured to determine the value of the interplanar spacings d [34]. The intensities of distinct bands discovered by the diffractometer, which finds the powder diffraction pattern, as well as the d values obtained from it, help to identify an unknown substance.
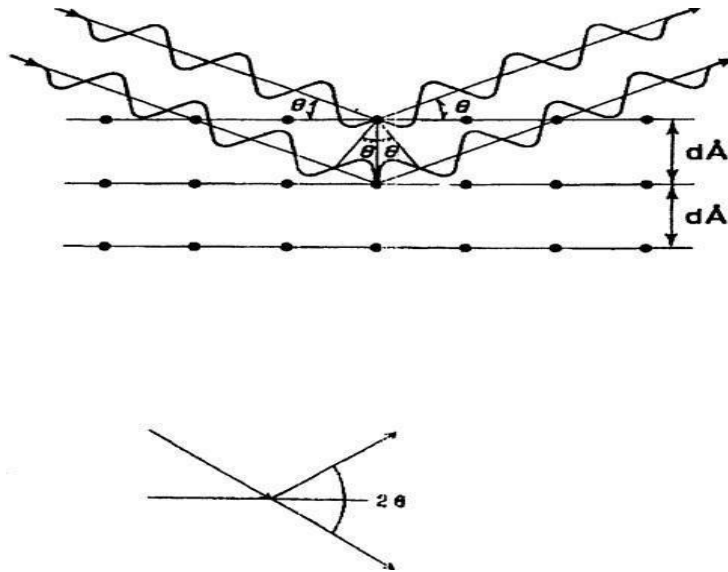
Fig. 2.8 Working principle of Bragg's law.

The data is then compared to the standardized line patterns for various composites in the PDF database. The three most extreme particular lines matched to the approved PDF model can be used to show the crystallinity of a sample that is present in uniform matter or in inhomogeneous solution. The distinction between conceivable phases can be performed by studying the distinct characteristic lines in particular subjects.

2.4.2   JCPDS

In 1941, the Joint Committee on Powder Diffraction Standards (JCPDS) was established. It maintains the Powder Diffraction File (PDF), which contains information on powder diffraction models such as relative intensities of conspicuous diffraction peaks and d-spacings. It is typically used to classify materials based on x-ray diffraction data and is intended for application. The International Centre for Diffraction Data (ICDD) is the name given to it currently. Every data set contains diffraction, sampling requirements, and bibliographic information, as well as device, laboratory, crystallographic, and desirable mechanical parameters in a standard graded style.

3.1 XRD of Pure KNN Calcined at 1050 °C

Fig. 3.1 shows the XRD pattern of $(K_{0.5}N_{0.5})NbO_3$ calcined at 1050 °C for 4 h.

The sample was prepared and data was compared to the JCPDS card number, 98-024-7574. XRD result shows that pure KNN possess single perovskite phase. That means all the ions diffused to from single crystal lattice. Also, the crystal structure found out to be tetragonal with space group P4mm and space group number 99.
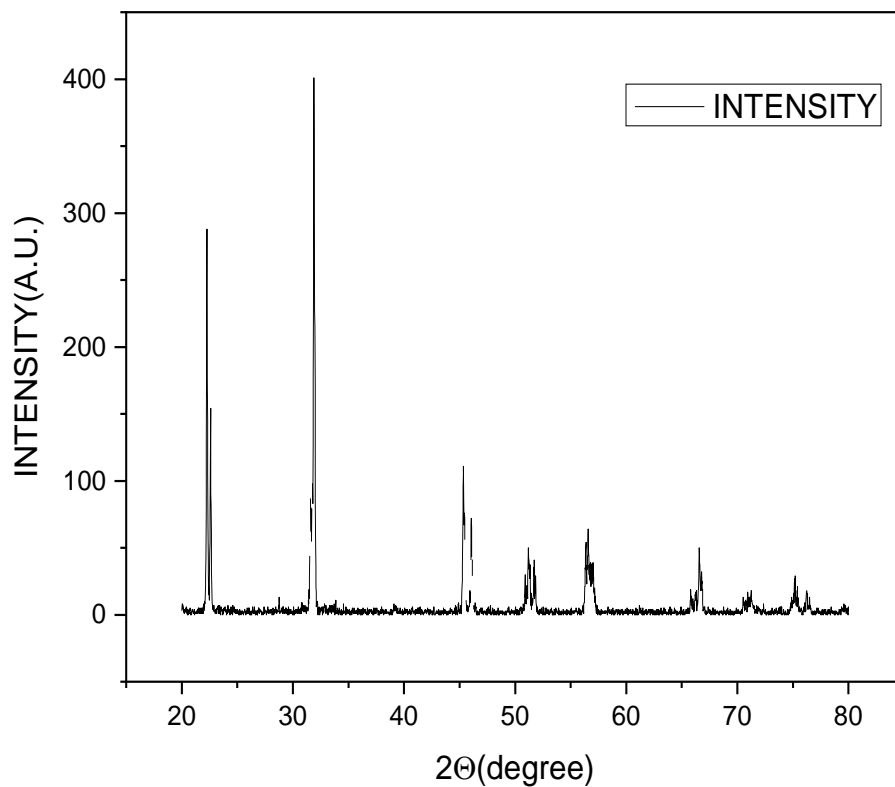

Fig. 3.1 XRD pattern of pure $(K_{0.5}N_{0.5})NbO_3$ Calcined at 1050 °C.

3.2 XRD of KNN: xHo (x= 0, 0.1, 0.5, 1, 2, 4) Ceramics

Fig. 3.2 shows the XRD pattern of KNN: xHo (x=0, 0.1, 0.5, 1, 2, 4) ceramics calcined at 1050 ºC for 4 h. All doped ceramics possess pure perovskite structure without any impurities, and no secondary structure is observed on the 2θ range of 20-80°, indicating that doped Ho^{3+} ion diffused into KNN lattice and a stable solid solution is formed. The radius of doped Ho^{3+} (1.22 Å) is comparable to the host ions K^+ (1.64 Å) and Na^+ (1.39 Å), therefore, doped Ho^{3+} will occupy the A-site of ABO_3 perovskite structure [27]. At elevated temperature the host ions K^+ and Na^+ volatilize from KNN which led to the defects and oxygen vacancies in KNN ceramics [18]. As Ho^{3+} ion occupies the A-site this will lead to the temperature stability of the KNN ceramics.
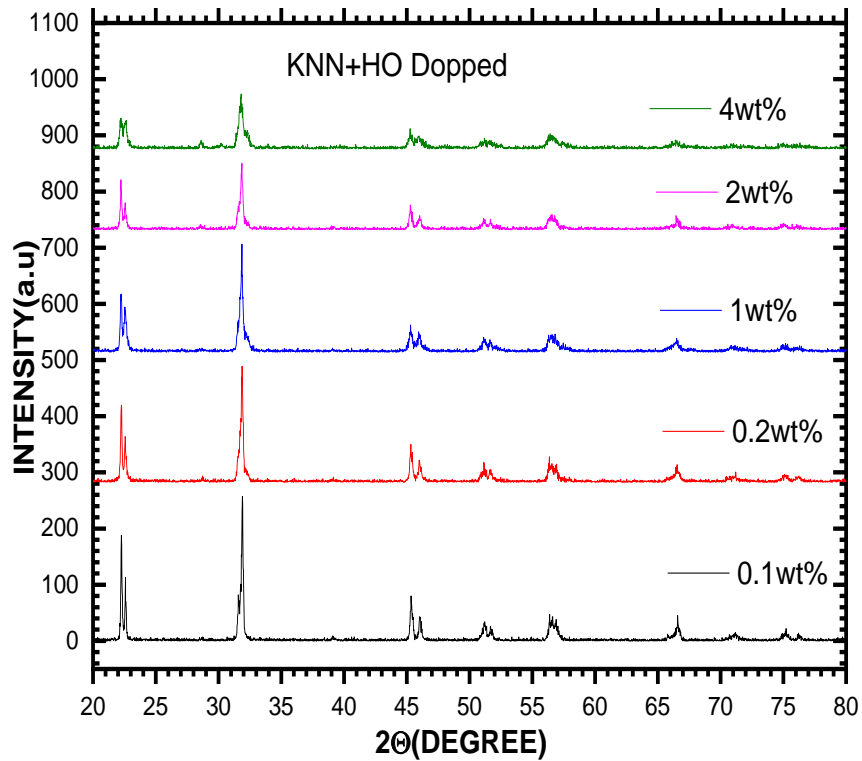

Fig. 3.2 XRD pattern of the KNN: xHo (x= 0, 0.1, 0.5, 1, 2, 4) ceramics.

CHAPTER 4

CONCLUSION

With a growing scarcity of renewable resources and a significant rise in energy demand, energy storage and use have become highly important. Energy harvesting from alternative energy sources is becoming increasingly important as a means of overcoming the demand rate, and substantial research is ongoing to find a sustainable solution to the energy crises. Mechanical energy is a key sustainable energy source that uses the piezoelectric effect to turn abundant ambient energy into usable power. PEGs have attracted a lot of attention in recent energy research because of their impressive levels of electro - mechanical conversion, which make them viable for a wide range of integrated applications. Piezoelectric energy harvesters now have wide variety of applications in day-to-day life such as in artificial pacemakers, SONAR systems, anti-lock brake system, transducers, and actuators etc. PZT and different doped modified forms, which display outstanding piezoelectric capabilities, are the most common piezoelectric materials. Pb-based materials will, however, be severely constrained in their application in the future due to the negative effects of Pb-elements on human health and the environment. As a result, it is vital to examine high performance materials that are environmentally safe (Pb-free). Various types of lead-free piezoelectric materials, including as BT, BNT, KNN, and PVDF, have recently been investigated and exhibit a number of benefits, along with good piezoelectricity, a simple structure, ease of synthesis, low manufacturing costs, and appropriateness for mass manufacturing and application. Among these piezoelectric materials KNN-based piezoceramics show promising piezoelectric, dielectric and ferroelectrics properties. Rare-earth ion doping is one such method which are used to improve properties of these KNN-based materials. So, in this study a lead free $(K_{0.5}N_{0.5})NbO_3$: xHo (x=0, 0.1, 0.5, 1, 2, 4) ceramics has been fabricated using solid-state reaction method. Calcined powders are then characterised for their structural properties using XRD characterization technique. The XRD pattern of Ho^{3+} doped $(K_{0.5}N_{0.5})NbO_3$ indicates that the obtained powder is in single phase. The thermal stability of the $(K_{0.5}N_{0.5})NbO_3$ ceramics was achieved by Ho3+ ions occupying the A-site of the ABO_3 perovskite structure.

FUTURE SCOPE

Calcined pure KNN and Ho doped KNN will be sintered at optimized temperature and will be characterized for microstructural, dielectric, ferroelectric properties and for piezoelectric energy harvesting application.

REFERNCES

[1]   E. Spain and A. Venkatanarayanan, "Review of Physical Principles of Sensing and Types of Sensing Materials," in *Comprehensive Materials Processing*, vol. 13, Elsevier Ltd, 2014, pp. 5–46. doi: 10.1016/B978-0-08-096532-1.01302-9.

[2]   S. M. Said, M. F. M. Sabri, and F. Salleh, "Ferroelectrics and Their Applications," in *Reference Module in Materials Science and Materials Engineering*, Elsevier, 2017. doi: 10.1016/b978-0-12-803581-8.04143-6.

[3]   K. C. Kao, "2 Electric Polarization and Relaxation," *Dielectric Phenomena in Solids* , 2004, doi: doi:10.1016/b978-012396561-5/50012-8.

[4]   T. Zheng, J. Wu, D. Xiao, and J. Zhu, "Recent development in lead-free perovskite piezoelectric bulk materials," *Progress in Materials Science*, vol. 98. Elsevier Ltd, pp. 552–624, Oct. 01, 2018. doi: 10.1016/j.pmatsci.2018.06.002.

[5]   J. Hao, W. Li, J. Zhai, and H. Chen, "Progress in high-strain perovskite piezoelectric ceramics," *Materials Science and Engineering R: Reports*, vol. 135. Elsevier Ltd, pp. 1–57, Jan. 01, 2019. doi: 10.1016/j.mser.2018.08.001.

[6]   A. Mayeen and N. Kalarikkal, "Development of ceramic-controlled piezoelectric devices for biomedical applications," in *Fundamental Biomaterials: Ceramics*, Elsevier Inc., 2018, pp. 47–62. doi: 10.1016/B978-0-08-102203-0.00002-0.

[7]   D. Hu, M. Yao, Y. Fan, C. Ma, M. Fan, and M. Liu, "Strategies to achieve high performance piezoelectric nanogenerators," *Nano Energy*, vol. 55. Elsevier Ltd, pp. 288–304, Jan. 01, 2019. doi: 10.1016/j.nanoen.2018.10.053.

[8]   V. Jella *et al.*, "A comprehensive review of flexible piezoelectric generators based on organic-inorganic metal halide perovskites," *Nano Energy*, vol. 57. Elsevier Ltd, pp. 74–93, Mar. 01, 2019. doi: 10.1016/j.nanoen.2018.12.038.

[9]   C. A. Howells, "Piezoelectric energy harvesting," *Energy Conversion and Management*, vol. 50, no. 7, pp. 1847–1850, Jul. 2009, doi: 10.1016/j.enconman.2009.02.020.

[10]   Z. Yang, S. Zhou, J. Zu, and D. Inman, "High-Performance Piezoelectric Energy Harvesters and Their Applications," *Joule*, vol. 2, no. 4. Cell Press, pp. 642–697, Apr. 18, 2018. doi: 10.1016/j.joule.2018.03.011.

[11]   B. Jaffe, R. S. Roth, and S. Marzullo, "Piezoelectric properties of Lead zirconate-Lead titanate solid-solution ceramics [8]," *Journal of Applied Physics*, vol. 25, no. 6. pp. 809–810, 1954. doi: 10.1063/1.1721741.

[12]   A. A. Bokov and Z.-G. Ye, "Recent Progress in Relaxor Ferroelectrics with Perovskite Structure *," 2020. [Online]. Available: www.worldscientific.com

[13] J. F. Li, K. Wang, F. Y. Zhu, L. Q. Cheng, and F. Z. Yao, "(K, Na) NbO3-based lead-free piezoceramics: Fundamental aspects, processing technologies, and remaining challenges," *Journal of the American Ceramic Society*, vol. 96, no. 12, pp. 3677–3696, Dec. 2013, doi: 10.1111/jace.12715.

[14] L. H. Bac *et al.*, "Tailoring the structural, optical properties and photocatalytic behavior of ferroelectric Bi0.5K0.5TiO3 nanopowders," *Materials Letters*, vol. 164, pp. 631–635, Feb. 2016, doi: 10.1016/j.matlet.2015.11.086.

[15] Saito Y, Takao H, Tani T, Nonoyama T, Takatori K, and et al. Homma T, "Lead-free piezoceramics," *Nature*, vol. 432, no. 7013, pp. 81–84, Nov. 2004, doi: 10.1038/nature03008.

[16] P. C. Reshmi Varma, "Low-dimensional perovskites," in *Perovskite Photovoltaics: Basic to Advanced Concepts and Implementation*, Elsevier, 2018, pp. 197–229. doi: 10.1016/B978-0-12-812915-9.00007-1.

[17] S. Gupta, D. Maurya, Y. Yan, and S. Priya, "Development of KNN-based piezoelectric materials," in *Lead-Free Piezoelectrics*, vol. 9781441995988, Springer New York, 2013, pp. 89–119. doi: 10.1007/978-1-4419-9598-8_3.

[18] M. Akmal, M. Harttar, # Mohd, W. A. Rashid, and A. L. Amani Azlan, "PHYSICAL AND ELECTRICAL PROPERTIES ENHANCEMENT OF RARE-EARTH DOPED-POTASSIUM SODIUM NIOBATE (KNN): A REVIEW," 2015.

[19] H. E. Mgbemere, M. Hinterstein, and G. A. Schneider, "Structural phase transitions and electrical properties of (K xNa 1-x)NbO 3-based ceramics modified with Mn," *Journal of the European Ceramic Society*, vol. 32, no. 16, pp. 4341–4352, Dec. 2012, doi: 10.1016/j.jeurceramsoc.2012.07.033.

[20] J. Tellier, B. Malic, B. Dkhil, D. Jenko, J. Cilensek, and M. Kosec, "Crystal structure and phase transitions of sodium potassium niobate perovskites," *Solid State Sciences*, vol. 11, no. 2, pp. 320–324, Feb. 2009, doi: 10.1016/j.solidstatesciences.2008.07.011.

[21] J. Wu, D. Xiao, and J. Zhu, "Potassium-sodium niobate lead-free piezoelectric materials: Past, present, and future of phase boundaries," *Chemical Reviews*, vol. 115, no. 7. American Chemical Society, pp. 2559–2595, Apr. 08, 2015. doi: 10.1021/cr5006809.

[22] A. W. Hewat, "Cubic-tetragonal-orthorhombic-rhombohedral ferroelectric transitions in perovskite potassium niobate : neutron powder profile refinement of the structures," 1973.

[23] Dwivedi Sushmita, Pareek Tanvi, and Kumar Sunil, "Structure, dielectric, and piezoelectric properties of K0.5Na0.5NbO3-based lead-free ceramics _ Enhanced Reader," 2018.

[24] J. Zhou, Q. Ma, P. Wang, L. Cheng, and S. Liu, "Influence of rare-earth Nd, Dy, and Ho doping on structural and electrical properties of (Na0.53K0.47)0.942Li

0.058NbO3 based lead-free piezoceramics," *Ceramics International*, vol. 40, no. 1 PART B, pp. 2451–2459, 2014, doi: 10.1016/j.ceramint.2013.08.020.

[25] W. Li *et al.*, "High-temperature and long-term stability of Ho-doped potassium sodium niobate-based multifunctional ceramics," *Ceramics International*, vol. 47, no. 10, pp. 13391–13401, May 2021, doi: 10.1016/j.ceramint.2021.01.196.

[26] Y. Zhang *et al.*, "Reversible luminescence modulation of Ho-doped K0.5Na0.5NbO3 piezoelectrics with high luminescence contrast," *Journal of the American Ceramic Society*, vol. 101, no. 6, pp. 2305–2312, Jun. 2018, doi: 10.1111/jace.15389.

[27] J. Xing *et al.*, "Influence of different lanthanide ions on the structure and properties of potassium sodium niobate based ceramics," *Scripta Materialia*, vol. 177, pp. 186–191, Mar. 2020, doi: 10.1016/j.scriptamat.2019.10.036.

[28] S.-J. Cho, M.-J. Uddin, and P. Alaboina, "Chapter three - Review of Nanotechnology for Cathode Materials in Batteries," 2017. doi: 10.1016/B978-0-323-42977-1/00003-0.

[29] V. Kumar, S. P. Tiwari, O. M. Ntwaeaborwa, and H. C. Swart, "Luminescence properties of rare-earth doped oxide materials," in *Spectroscopy of Lanthanide Doped Oxide Materials*, Elsevier Inc., 2019, pp. 345–364. doi: 10.1016/B978-0-08-102935-0.00010-1.

[30] Y. Chen, "Carbon Nanotechnology Edited by Liming Dai Solid-state formation of carbon nanotubes," 2006.

[31] N. Gupta and B. Basu, "Hot pressing and spark plasma sintering techniques of intermetallic matrix composites," in *Intermetallic Matrix Composites*, Elsevier, 2018, pp. 243–302. doi: 10.1016/b978-0-85709-346-2.00010-8.

[32] A. Buekenhoudt, A. Kovalevsky, I. J. Luyten, and F. Snijkers, ."11 Basic Aspects in Inorganic Membrane Preparation."

[33] R. Kohli, "Developments in Imaging and Analysis Techniques for Micro- and Nanosize Particles and Surface Features," in *Developments in Surface Contamination and Cleaning: Detection, Characterization, and Analysis of Contaminants*, Elsevier Inc., 2012, pp. 215–306. doi: 10.1016/B978-1-4377-7883-0.00005-5.

[34] B. D. CULLITY, *Elements of X-Ray Diffraction*.